

HIGH POSITION RESOLUTION BPM READOUT SYSTEM WITH CALIBRATION PULSE GENERATORS FOR KEK e⁺/e⁻ LINAC

F. Miyahara[#], K. Furukawa, M. Satoh, Y. Seimiya, T. Suwada, KEK, Tsukuba, Ibaraki, Japan
 R. Ichimiya, JAEA, Rokkasho, Aomori, Japan
 H. Saotome, KIS, Tsuchiura, Ibaraki, Japan

Abstract

The KEK e⁺/e⁻ injector linac will be operated in multiple modes for the electron beam injection to three independent storage rings, the SuperKEKB HER, Photon Factory (PF) Ring and the PF-AR, and the positron beam injection into the damping ring and the SuperKEKB LER. The beam current ranges between 0.1 and 10 nC/bunch. The beam current depends on the beam mode. The operation modes can be switched every 20 milliseconds. The injector linac is under upgrade for the SuperKEKB, where the required resolution of beam position measurement is less than $\sigma=10\ \mu\text{m}$. However, the current beam position monitor (BPM) readout system based on oscilloscopes for stripline beam position monitors has the position resolution of $50\ \mu\text{m}$ approximately. Thus, we have developed a new BPM readout board with narrow band pass filter, 16-bit, 250 Msps ADCs and calibration pulse generators. The system is based on VME standard and the beam position is calculated by FPGA on board. The calibration pulse follows every position measurement. The calibration pulse is used for the gain correction and the integrity monitor of the cable connection. We will report details of the system.

INTRODUCTION

In the SuperKEKB, the injector linac is required to inject 5 nC/bunch, 7 GeV electron and 4 nC/bunch, 4 GeV positron beams with the emittance less than 20 mm-mrad. The electron beam with emittance of about 10 mm-mrad, is generated by a photocathode RF gun [1]. The initial emittance is low enough for the requirement, but an emittance growth due to the short range transverse wakefield which is caused by misalignment is not negligible. The emittance growth can be suppressed by using the offset injection method [2]. Numerical studies show the emittance at the end of the linac is less than 20 mm-mrad under the condition of alignment error of 0.1 mm [3,4]. To perform the offset injection in the linac, at least resolution of $10\ \mu\text{m}$ is required. However, the resolution of current oscilloscope based BPM readout system [5] is about $50\ \mu\text{m}$. The beam is also transported to the PF ring. The bunch charge for the PF ring is 0.2 nC/pulse during the top-up operation. By contrast, primary electron beam for positron production will be

10 nC/bunch. Those operation modes are switched every 20 ms. Thus, the wide dynamic range for beam currents is required. The dynamic range can be ensured by setting attenuation of the BPM signal for every beam modes or currents. That means several gain parameter sets and a calibration system to fix those parameters are needed. The calibration system allows the monitoring of a variation of the gain and integrity of the cable connection. The newly developed board was designed to have the high position resolution with dynamic range from 0.1 to 10 nC/bunch and to be equipped calibration pulse generators. A position resolution of $\sigma=3\ \mu\text{m}$ for 0.1 nC/bunch beam was achieved [6]. The board is also designed to have wide dynamic range for the position. The detail of the design is reported in previous studies [6,7]. There are 93 stripline BPMs on the linac, 20 VME crates with 3-8 readout boards are set on klystron gallery. The old system will be replaced with the new one stepwise after this summer. In this paper, we report a whole system of the BPM, calibration scheme and stability of the gain.

BPM SYSTEM

The BPM readout system consists of a VME CPU board (MVME5500), a RAS (Reliability, Accessibility, Serviceability) board, an Event Receiver (VME-EVR-230RF) [8] and BPM readout boards. An EPICS IOC [9] runs on the CPU. The RAS board monitor status (such as power, temperature) and control the fan of the VME crate. The event receiver is used for the distinction of the beam mode and the generation of triggers to BPM boards. The readout board has 4 signal input channels for one stripline BPM. The calibration signal is also sent from one of those channels to the corresponding electrode.

BPM Readout Board

The BPM readout board is composed of four RF units which detect the signal from BPM electrodes, 16-bit 250 MSPS ADCs, sub FPGAs for the ADC and a main FPGA. The position and charge of the beam are calculated in the main FPGA. Those results and parameters for the calculation and the operation of the board are recorded in the registers on main FPGA. Figure 1 shows the block diagram of the board and the RF unit. The setting value of the variable attenuator, sum of ATT1A and ATT1B, depends on bunch charge. In particular, the beam is away from BPM center, a nonlinearity of the ADC gain causes a measured position drift. The readout board has a good

[#]fusashi.miyahara@kek.jp

linearity, less than $\pm 5 \mu\text{m}$ drift in position, for the relative input signal of $\pm 10 \text{ dB}$.

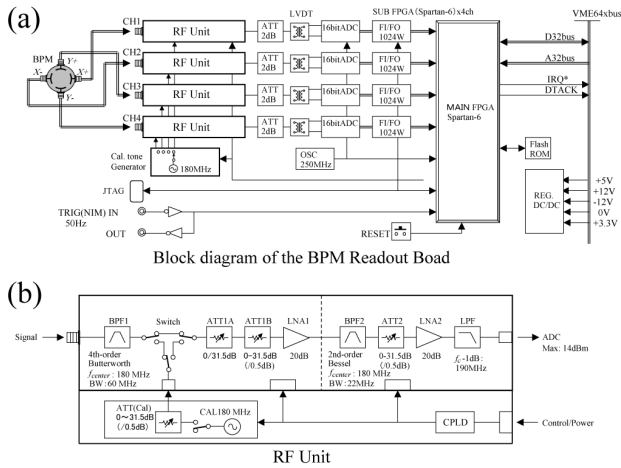


Figure 1: Schematics the BPM readout board (a) and the RF Unit (b).

The signal from the stripline BPM is filtered by 4th-order Butterworth filter which has a bandwidth (BW) of 60 MHz with center frequency (f_{center}) of 180 MHz and the 2nd-order Bessel filter ($BW = 22 \text{ MHz}$, $f_{center} = 180 \text{ MHz}$). The double bunch operation with time interval of 96 ns is required in the operations for SuperKEKB. Thus, the Bessel filter is used to convert a bipolar signal to ringing sinusoidal waveform with full-width of $\sim 90 \text{ ns}$. The Butterworth filter is used to compensate rather broad cut-off characteristic of the Bessel filter. The beam position is given by,

$$x = A_0 + \sum_{m=0}^3 \sum_{n=0}^3 a_{mn} (\Delta_H / \Sigma_H)^m (\Delta_V / \Sigma_V)^n \quad (1)$$

$$y = B_0 + \sum_{m=0}^3 \sum_{n=0}^3 b_{mn} (\Delta_H / \Sigma_H)^m (\Delta_V / \Sigma_V)^n,$$

where

$$\Delta_H = W_1 - W_2, \Sigma_H = W_1 - W_2 \quad (2)$$

$$\Delta_V = W_3 - W_4, \Sigma_H = W_3 - W_4$$

$$W_i = G_i G'_i \sqrt{\sum_j (V_{i,j} - V_{i,ped})^2}. \quad (3)$$

The coefficients a_{mn} and b_{mn} were given by fitting the function to the mapping data taken from stretched wire measurement. The variables A_0 and B_0 stand for the offset of electrical center from the quadrupole magnet center and are determined by beam based alignment. An output signal from an electrode is given by root sum square of ADC values within a window which covers the beam/calibration signal and correction factor G and G' . The variable $V_{i,j}$ and $V_{i,ped}$, are ADC value of the i -th electrode (see Fig. 1), where j represents ADC channel, and the pedestal, respectively. The factor G stands for

ISBN 978-3-95450-176-2

static signal balance between electrodes and depends on signal attenuation in the coaxial cable and a variation of circuit element. The G' , dynamic gain factor, represents gain drift which strongly depends on the environmental temperature. Those factors are discussed in the next section.

Calibration Pulse

The calibration pulse is used for a correction of gain balance between electrodes and a monitor of gain drift and cable connection. The signal is shown in Fig. 2. The signal is sent to one of the four electrodes, and then return signals are measured by the readout system. Figure 3 shows ADC signals for the output pulse which was sent from Ch1. Both Ch3 and Ch4 correspond to adjoining electrodes and detect large signal at around 2400 ns. The small signal after the large signal, delayed about 350 ns, represents reflection. The calibration pulse can be set from a short pulse to CW. The pulse width is controlled by the switch after the RF module. Due to response to the CW contains superposition of reflection signals; a short pulse is adopted for the calibration. The attenuator after the calibration module, ATT(CAL) in Fig. 1, is used to avoid saturation of the amplifiers and ADC. The power of the RF at the BPF1 input is 36 dBm in ATT(CAL)=0 dB. In case of a largest attenuation setting which corresponds to 10 nC/bunch, we confirmed that signal level enough for the calibration can be obtained.

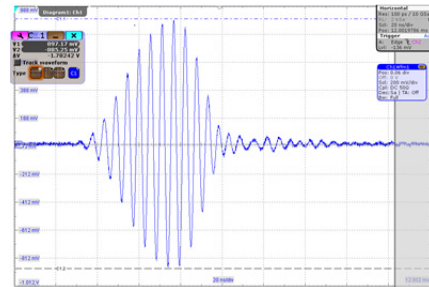


Figure 2: Calibration pulse signal.

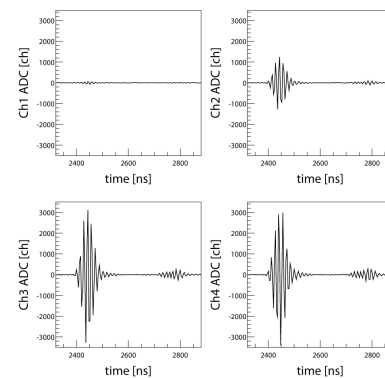


Figure 3: ADC response to the calibration pulse. The pulse was sent to the BPM from Ch1(X+).

Control and Operation

The readout system is controlled by EPICS framework which was utilized for most devices in the injector linac. The EPICS IOC works on VxWorks 5.5.1. All parameters for the operation and results of a measurement such as position, charge and waveform can be taken from EPICS records. To reduce data acquisition (DAQ) time, the waveform of the signal is not transferred in normal operation. It takes about 3.5 ms to take four waveforms in the board. The waveform is used for setting/confirming the ADC gate. The development of the software is ongoing. The detail of the software will be reported in elsewhere [10].

DAQ scheme is the following:

1. External Trigger
 - Beam Data acquisition
 - Writing parameters for calibration
2. Internal Trigger (6.6 ms after the ext. trigger)
 - Calibration Data acquisition for Horizontal
 - Writing parameters for calibration
3. Internal Trigger (13.2 ms after the ext. trigger)
 - Data acquisition for calibration (vertical)
 - Writing parameters for a next beam.

The external triggers are synchronized the beam timing which is distributed by the EVR. The writing parameter required for each process because parameters such as attenuation setting, gain factor could be changed. The repetition rate of the linac is 50 Hz; three DAQ processes are performed in 20 ms interval. Thus, one DAQ process must be less than 6 ms. Figure 4 shows total elapsed times for one DAQ process in case of maximum load with 8 readout boards. The DAQ time is much faster than required time.

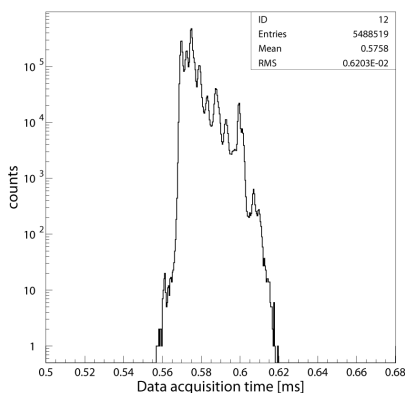


Figure 4: Total elapsed time for one data acquisition process with 8 BPM readout boards.

SIGNAL STABILITY AND GAIN BALANCE

Studies of the gain drift and gain balance between opposite electrodes have been performed by using the calibration pulse. The drift of signal level and gain

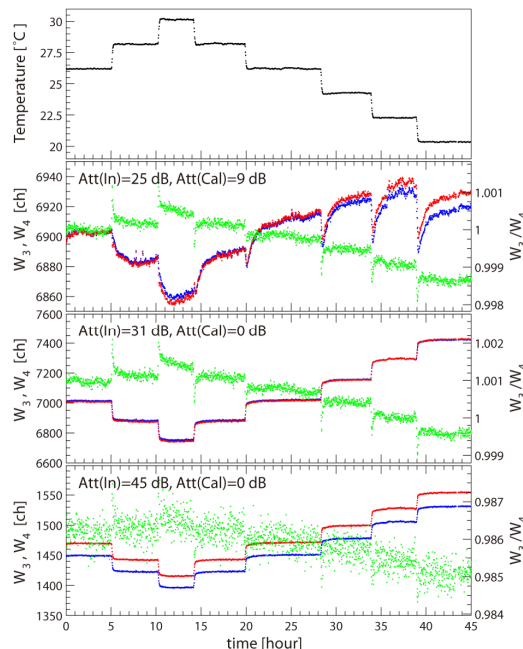


Figure 5: Signal level and gain balance variation. Temperature is shown in the top. Signal levels of CH3(Y+) and CH4(Y-) are plotted by red and blue dots, respectively. The green dots show the ratio of both signals. The Att(In) and Att(Cal) stand for attenuation value for the input (ATT1A+ATT1B) and output of the calibration.

balance lead to variation of measured charge and position, respectively. The gain balance reflects variation in circuit elements. In particular, the amplifier has a rather large temperature-dependence compared with other elements. Thus, the temperature dependence of the system and the gain drift has been studied. The response to the calibration signals for different environmental temperatures measured by putting a BPM, 30 m coaxial cables and the readout system in a thermostatic chamber. The signal level W_3 , W_4 and gain balance W_3/W_4 for the calibration pulse from CH1 are plotted with the temperature in Fig. 5. Where, $G = G' = 1$ in Eq. 3. Three sets of the attenuation settings correspond to different bunch charge, 0.5, 1 and 5 nC/bunch. In case of Att(In)=25 dB, in order to keep the signal level to be in good linearity region, the attenuator just after the pulse generator was set to 9 dB. Each data point shown in Fig. 5 is an average of 500 events, and a statistical error is less than 1 ch. The environmental temperature was changed every ~5 hours. The signal and gain balance are very stable and shows quick response and good reproducibility to the temperature, except in the case 9 dB attenuation for the calibration pulse. It appears that the attenuator needs much more time to be an equilibrium state due to high output power of the pulse generator. This variation is less than 1% and the absolute value of the signal does not affect the beam position but the charge. The temperature dependence of the signal level is $-1\%/^{\circ}\text{C}$ in the system.

Figure 6 shows temperature dependence of the gain balance. The data are averages of 10 minutes just before changing the temperature setting. It has been found that the temperature dependence of the gain is very small, less than 0.02%/°C which corresponds to about 1 $\mu\text{m}/^\circ\text{C}$, and shows same gradient for different attenuation settings. In the injector linac, the room temperature is kept in 23 to 26 °C. As a result, the position drift due to a temperature fluctuation is negligible and a correction of the gain drift, G' , is not required. By contrast, the value of the gain balance depends on the attenuation value, Att(In), that corresponds the beam charge. The static gain factor G will be set so that the signal ratio of opposite electrodes becomes 1 for any attenuation setting. The calibration pulse can be powerful equipment to perform the gain calibration in our linac. More precise gain correction can be performed by using the beam.

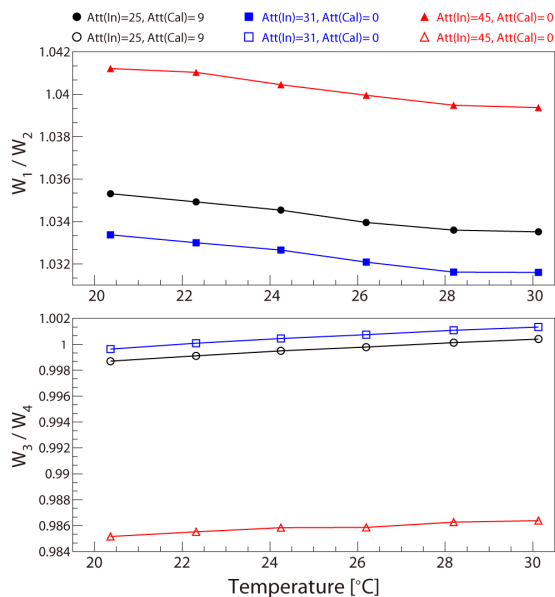


Figure 6: The gain ratio vs. the environmental temperature.

CONCLUSION

In order to suppress the emittance growth in the KEK e+/e- linac, a new BPM system with high position resolution and wide dynamic range in beam charge and position is required. We have developed the new VME-based BPM readout system which consists of CPU board, RAS board, EVR for event timing system and the new readout board with a calibration pulse generator. The system shows negligible gain drift, less than 1 μm , in the

environmental temperature of the injector linac. The calibration system gives easy ways to correct the gain balance for any attenuation settings that correspond to beam currents.

ACKNOWLEDGMENT

We greatly thank Dr. Steve Smith (SLAC) and Dr. Andrew Yang (SLAC) for providing us with the important information of the developing of BPM readout system and meaningful suggestions. The authors would like to express thank to Dr. Makoto Tobiyama (KEK) for useful suggestions. We grateful Kyosuke Yamada (DIGITEX LAB. CO.) for his support in the fabrication of the readout board.

REFERENCES

- [1] T. Natsui et al., “Quasi-Traveling Wave RF Gun and Beam Commissioning for SuperKEKB”, TUPJE003, IPAC’15, Richmond, Virginia, USA (2015).
- [2] A.W. Chao, B. Richter and C.Y. Yao, Nucl. Instrum. Methods 178, 1(1980).
- [3] M. Satoh, “Injector commissioning”, The 19th KEKB Accelerator Review Committee, KEK, Tsukuba, Japan (2014); <http://www-kekb.kek.jp/MAC/2014>.
- [4] S. Kazama et al., “Emittance Preservation in SuperKEKB Injector”, MOPWA071, IPAC’15, Richmond, Virginia, USA (2015).
- [5] M. Satoh et al., “EPICS IOC of WindowsXP-based Oscilloscope for Fast BPM Data Acquisition System”, WEP086, ICALEPCS2009, Kobe, Japan (2009).
- [6] R. Ichimiya et al., “Development of High Precision Beam Position Monitor Readout System with Narrow Bandpass Filters for the KEKB Injector Linac towards the SuperKEKB”, WEPC14, IBIC2013, Oxford, UK (2013).
- [7] R. Ichimiya et al., “High Position Resolution and High Dynamic Range Stripline Beam Position Monitor (BPM) Readout System for the KEKB Injector Linac Towards the SuperKEKB”, WEPD04, IBIC2014, Monterey, USA (2014).
- [8] Micro-Research Finland Oy website: <http://www.mrf.fi>
- [9] Experimental Physics and Industrial Control System: website: <http://www.aps.anl.gov/epics/>
- [10] M. Satoh et al., “Development of BPM Readout System for SuperKEKB Injector Linac”, MOPGF034, ICALEPCS2015, Melbourne, Australia (2015).